Pramāṇa, Vol. 8, No. 3, 1977, pp. 229–244. © Printed in India.

Charged particle trajectories in a magnetic field on a curved space-time

A R PRASANNA and R K VARMA
Physical Research Laboratory, Ahmedabad 380009

MS received 3 November 1976; in revised form 10 January 1977

Abstract. In this paper we have studied the motion of charged particles in a dipole magnetic field on the Schwarzschild background geometry. A detailed analysis has been made in the equatorial plane through the study of the effective potential curves. In the case of positive canonical angular momentum the effective potential has two maxima and two minima giving rise to a well-defined potential well near the event horizon. This feature of the effective potential categorises the particle orbits into four classes, depending on their energies. (i) Particles, coming from infinity with energy less than the absolute maximum of V_{eff}, would scatter away after being turned away by the magnetic field. (ii) Whereas those with energies higher than this would go into the central star seeing no barrier. (iii) Particles initially located within the potential well are naturally trapped, and they execute Larmor motion in bound gyrating orbits. (iv) and those with initial positions corresponding to the extrema of V_{eff} follow circular orbits which are stable for non-relativistic particles and unstable for relativistic ones. We have also considered the case of negative canonical angular momentum and found that no trapping in bound orbits occur for this case.

In the case when particles are not confined to the equatorial plane we have found that the particles execute oscillatory motion between two mirror points if the magnetic field is sufficiently high, but would continuously fall towards the event horizon otherwise.

Keywords. Charged particle orbits; black holes; pulsars; general relativity.

1. Introduction

Recent advances in x-ray and radio astronomy have revealed some very interesting structure of various x–ray and radio sources. Whereas the identification of pulsars as rotating neutron stars (ter Haar 1972) is by and large considered established, the suggestion that the cygnus X-1 may be an accreting black hole with a companion giant star is still on the side of speculation and needs a more detailed and careful analysis (IAU Symposium 1974).

The mechanism of radiation which constitutes the pulses observed from pulsars is not well understood, while much less is known about the dynamics of accretion of matter onto the black hole, which is suggested to be the mechanism of x-ray

emission. One suggestion which seems most reasonable is that these radiation emissions are due to plasma processes near such astrophysical objects like neutron stars and black holes (Thorne and Novikov 1972, Zeldovich and Novikov 1973). Most of these astronomical objects are believed to have strong magnetic fields associated with them. Since these objects are quite massive ($\gtrsim 1\ M_\odot$) the gravitational field associated with them should necessarily be treated general relativistically in the sense of considering the space-time curvature associated with them. Hence it is most desirable to consider the dynamics of relativistic plasmas in the presence of a strong magnetic field on the curved space-time of the central body.

With this study in mind we first consider the dynamics of a charged particle in a dipole magnetic field on the curved background, of a non-rotating central body without any charge. So far, no exact solution of Einstein-Maxwell equations has been found which is asymptotically flat, has *non-zero* magnetic dipole moment, but zero total charge, zero total magnetic monopole moment and zero total angular momentum.* However, rather than look for exact solutions, we follow Ginzburg and Ozernoi (1964) and assume that the magnetic field energy is small so that its effect on the curvature may be neglected in comparison with that of the mass of the central body. As shown by the above authors, the background Schwarzschild geometry modifies the components of the dipole magnetic field. With this background, we study in this paper the motion of a charged particle in the presence of the modified magnetic dipole field on the Schwarzschild space-time, through the usual geodesic equations including the Lorentz force terms.

In section 2, we obtain the components of the modified electromagnetic field tensor F_{ij} on Schwarzschild background and in section 3 the equations of motion are presented through a Lagrangian approach. Section 4 gives a detailed analysis of the nature of the orbits in the equatorial plane through the study of the effective potential curves and this is followed in section 5 by the actual evaluation of few orbits in the equatorial plane as well as motion along the field lines. Finally we have drawn few conclusions, which naturally suggest that in subsequent work we shall consider the motion of the guiding centre (centre of the Larmor circle for a particle gyrating in a magnetic field) on a curved background geometry which is an essential step for considering plasma-processes.

2. Evaluation of field components

The background curved space-time is given by the Schwarzschild metric

$$ds^2 = -\left(1-\frac{2m}{r}\right)^{-1} dr^2 - r^2 d\theta^2 - r^2 \sin^2\theta\, d\phi^2 + \left(1-\frac{2m}{r}\right) c^2 dt^2 \tag{2.1}$$

where $m = MG/c^2$, M being the total mass of the source. We assume a dipole magnetic field which expressed in local Lorentz frame, has the components

$$F_{(\theta\phi)} = B_r = \frac{2\mu\cos\theta}{r^3} f(r),$$

*We wish to thank K S Thorne and W Kinnersley for a correspondence regarding this question.

$$F_{(\phi r)} = B_\theta = \frac{\mu \sin \theta}{r^3} g(r),$$

$$F_{(r\theta)} = B_\phi = 0, \tag{2.2}$$

wherein μ is the magnetic moment and $f(r)$ and $g(r)$ are two arbitrary functions which shall eventually represent the curvature effects in the magnetic field. The components of the orthonormal tetrad $\lambda_i^{(\alpha)}$ of the local Lorentz frame for Schwarzschild geometry are given by

$$\lambda_1^{(1)} = \left(1 - \frac{2m}{r}\right)^{-\frac{1}{2}}, \qquad \lambda_2^{(2)} = r$$

$$\lambda_3^{(3)} = r \sin \theta, \qquad \lambda_4^{(4)} = \left(1 - \frac{2m}{r}\right)^{\frac{1}{2}}. \tag{2.3}$$

Hence the components of the electromagnetic field tensor F_{ij} defined in the Schwarzschild frame through,

$$F_{ij} = \lambda_i^{(\alpha)} \lambda_j^{(\beta)} F_{(\alpha\beta)} \tag{2.4}$$

are given by

$$F_{\theta\phi} = \frac{2\mu \sin \theta \cos \theta}{r} f(r),$$

$$F_{\phi r} = \mu \left(1 - \frac{2m}{r}\right)^{-\frac{1}{2}} \frac{\sin^2 \theta}{r^2} g(r),$$

$$F_{r\theta} = 0. \tag{2.5}$$

In order to determine f and g, we now solve the Maxwell's equations, which in the absence of currents and charges are given by

$$F_{ij}^{ij} = 0, \quad F_{ij,k} + F_{jk,i} + F_{ki,j} = 0. \tag{2.6}$$

Using the components of F_{ij} as given by (2.5) and the metric components (2.1), we get the equations

$$\frac{d}{dr}(f/r) + \frac{g}{r^2\left(1 - \frac{2m}{r}\right)^{\frac{1}{2}}} = 0,$$

$$\frac{d}{dr}\left[\frac{\left(1 - \frac{2m}{r}\right)^{\frac{1}{2}} g}{r^2}\right] + \frac{2f}{r^3} = 0. \tag{2.7}$$

Ginzburg and Ozernoi (1964) have solved the same set of equations while considering the external field of a magnetic star and we take their solution as given by

$$f = -\frac{3r^3}{8m^3}\left[\ln\left(1 - \frac{2m}{r}\right) + \frac{2m}{r}\left(1 + \frac{m}{r}\right)\right],$$

$$g = \frac{3r^2}{4m^2}\left[\left(1-\frac{2m}{r}\right)^{-1} + \frac{r}{m}\ln\left(1-\frac{2m}{r}\right) + 1\right]. \tag{2.8}$$

With these we have the non-zero components of F_{ij} as given by

$$F_{\phi r} = \frac{3\mu \sin^2\theta}{4m^2}\left[\left(1-\frac{2m}{r}\right)^{-1} + \frac{r}{m}\ln\left(1-\frac{2m}{r}\right) + 1\right]\left(1-\frac{2m}{r}\right)^{V_2}$$

$$F_{\phi\theta} = \frac{3\,\mu \sin\theta\cos\theta}{4m^3} r^2\left[\ln\left(1-\frac{2m}{r}\right) + \frac{2m}{r}\left(1+\frac{m}{r}\right)\right]. \tag{2.9}$$

Using the definition $F_{ij} = (A_{j,i} - A_{i,j})$ for the vector potential A_i, we can now solve it from the components of F_{ij} and we get

$$A_i = (0, 0, A_\phi, 0)$$

with

$$A_\phi = -\frac{3\mu \sin^2\theta}{8m^3}\left[r^2 \ln\left(1-\frac{2m}{r}\right) + 2mr + 2m^2\right]. \tag{2.10}$$

The above expression for the vector potential is obtained with the assumption that the magnetic moment μ is that of a point dipole situated at the origin $r = 0$ rather than being distributed over the region of the central body. Petterson (1974) has considered the magnetic field surrounding a Schwarzschild black hole arising out of current loops around the black hole and he finds that the magnetic dipole moment tends to zero as the radius of the loop shrinks to $r = 2m$. However, for the purpose of our consideration, *viz.*, finding the orbits of the charged particles, we shall keep away from the event horizon and shall determine the trajectories in the region $r > 2m$. Our consideration may thus be better applicable to a central body with radius $> 2m$ rather than to a black hole.

3. Equations of motion

The Lagrangian for the motion of a charged particle of charge e and mass M_0 is given by

$$\mathcal{L} = \tfrac{1}{2}\Big\{c^2(1-2m/r)\,\dot{t}^2 - (1-2m/r)^{-1}\dot{r}^2 - r^2\dot{\theta}^2 - r^2\sin^2\theta\,\dot{\phi}^2$$

$$+ \frac{3e\mu\sin^2\theta}{4M_0c^2m^3}\left[r^2\ln(1-2m/r) + 2mr + 2m^2\right]\dot{\phi}\Big\} \tag{3.1}$$

where an overhead dot denotes differentiation with respect to the proper time s.

Since the dipole magnetic field is axisymmetric and the background geometry is spherically symmetric, we see that the Lagrangian is independent of the azimuthal coordinate ϕ. Furthermore, as both the fields considered are static, the Lagrangian is also independent of t. These two symmetries give rise to two integrals of motion, the canonical angular momentum h and the total energy K respectively. We thus have corresponding to the coordinates ϕ and t,

$$\partial \mathcal{L}/\partial \dot{\phi} \equiv$$

$$r^2 \sin^2\theta \frac{d\phi}{ds} - \frac{3e\mu r^2 \sin^2\theta}{8M_0c^2m^3}\left[\ln\left(1-\frac{2m}{r}\right)+2m\left(1+\frac{m}{r}\right)\right]=h \tag{3.2}$$

and

$$\frac{\partial \mathcal{L}}{\partial \dot{t}} \equiv c\left(1-\frac{2m}{r}\right)\frac{dt}{ds}=K. \tag{3.3}$$

The equations of motion corresponding to r and θ coordinates are given by

$$\frac{d^2r}{ds^2}-\frac{m}{r^2}\left(1-\frac{2m}{r}\right)^{-1}\left(\frac{dr}{ds}\right)^2-r\left(1-\frac{2m}{r}\right)\left\{\left(\frac{d\theta}{ds}\right)^2+\sin^2\theta\left(\frac{d\phi}{ds}\right)^2\right\}$$

$$+\frac{mc^2}{r^2}\left(1-\frac{2m}{r}\right)\left(\frac{dt}{ds}\right)^2=-\frac{3e\mu\sin^2\theta}{2M_0c^2m^3}\left[\left(1-\frac{m}{r}\right)\right.$$

$$\left.+\left(\frac{r}{2m}-1\right)\ln\left(1-\frac{2m}{r}\right)\right]\left(\frac{d\phi}{ds}\right). \tag{3.4}$$

$$\frac{d^2\theta}{ds^2}+\frac{2}{r}\frac{dr}{ds}\frac{d\theta}{ds}-\sin\theta\cos\theta\left(\frac{d\phi}{ds}\right)^2=-\frac{3e\mu\sin\theta\cos\theta}{4M_0c^2m^3}$$

$$\times\left[\frac{2m}{r}\left(1+\frac{m}{r}\right)+\ln\left(1-\frac{2m}{r}\right)\right]\left(\frac{d\phi}{ds}\right) \tag{3.5}$$

As the orbit equations involve transcendental functions, it is almost analytically impossible to make any general analysis. Hence we resort to numerical integration and get certain qualitative picture of the nature of the orbits for different values of the physical parameters appearing in the equations. For convenience of calculations we shall consider the equations in dimensionless form by introducing the dimensionless quantities.

$$\rho=\frac{r}{m},\ \sigma=\frac{s}{m},\ H=\frac{h}{m},\ \lambda=\frac{e\mu}{M_0c^2m^2}. \tag{3.6}$$

With these definitions the equations of motion read as:

$$\frac{d^2\rho}{d\sigma^2}-\frac{1}{\rho^2}\left(1-\frac{2}{\rho}\right)^{-1}\left[\left(\frac{d\rho}{d\sigma}\right)^2-K^2\right]-(\rho-2)\left[\left(\frac{d\theta}{d\sigma}\right)^2+\sin^2\theta\left(\frac{d\phi}{d\sigma}\right)^2\right]$$

$$=-\frac{3\lambda\sin^2\theta}{2}\left[\left(1-\frac{1}{\rho}\right)+\left(\frac{\rho}{2}-1\right)\ln\left(1-\frac{2}{\rho}\right)\right]\left(\frac{d\phi}{d\sigma}\right) \tag{3.7}$$

$$\frac{d^2\theta}{d\sigma^2}+\frac{2}{\rho}\frac{d\rho}{d\sigma}\frac{d\theta}{d\sigma}-\sin\theta\cos\theta\left(\frac{d\phi}{d\sigma}\right)^2=-\frac{3\lambda\sin\theta\cos\theta}{4}$$

$$\times\left[\ln\left(1-\frac{2}{\rho}\right)+\frac{2}{\rho}\left(1+\frac{1}{\rho}\right)\right]\left(\frac{d\phi}{d\sigma}\right) \tag{3.8}$$

$$\frac{d\phi}{d\sigma} = \frac{H}{\rho^2 \sin^2 \theta} + \frac{3\lambda}{8}\left[\ln\left(1-\frac{2}{\rho}\right) + \frac{2}{\rho}\left(1+\frac{1}{\rho}\right)\right] \tag{3.9}$$

and

$$1 = \left(1-\frac{2}{\rho}\right)^{-1}\left[K^2 - \left(\frac{d\rho}{d\sigma}\right)^2\right] - \rho^2\left[\left(\frac{d\theta}{d\sigma}\right)^2 + \sin^2\theta\left(\frac{d\phi}{d\sigma}\right)^2\right] \tag{3.10}$$

wherein we have used eq. (3.3) to eliminate dt/ds in (3.4) to get (3.7) and in the metric (2.1) to get (3.10).

4. Motion in the equatorial plane

We first specialize to the case of the motion in the equatorial plane defined by $\theta = \pi/2$, $d\theta/d\sigma = 0$. From (3.8) we get $(d^2\theta/d\sigma^2) = 0$, showing that the particle will be confined to the equatorial plane. Rest of the equations take the form

$$\frac{d^2\rho}{d\sigma^2} - \frac{1}{\rho^2}\left(1-\frac{2}{\rho}\right)^{-1}\left[\left(\frac{d\rho}{d\sigma}\right)^2 - K^2\right] - (\rho-2)\left(\frac{d\phi}{d\sigma}\right)^2$$

$$= -\frac{3\lambda}{2}\left[\left(1-\frac{1}{\rho}\right) + \left(\frac{\rho}{2}-1\right)\ln\left(1-\frac{2}{\rho}\right)\right]\left(\frac{d\phi}{d\sigma}\right), \tag{4.1}$$

$$\frac{d\phi}{d\sigma} = \frac{H}{\rho^2} + \frac{3\lambda}{8}\left[\ln\left(1-\frac{2}{\rho}\right) + \frac{2}{\rho}\left(1+\frac{1}{\rho}\right)\right] \tag{4.2}$$

and

$$\left(\frac{d\rho}{d\sigma}\right)^2 + \left(1-\frac{2}{\rho}\right)\left[1+\rho^2\left(\frac{d\phi}{d\sigma}\right)^2\right] = K^2. \tag{4.3}$$

It can be easily verified (with some algebra) that the energy expression in (4.3) is an exact integral of (4.1), and thus we can confine our attention to eqs (4.2) and (4.3). Substituting for $d\phi/d\sigma$ from (4.2) in (4.3) we get,

$$K^2 = \left(\frac{d\rho}{d\sigma}\right)^2 - \left(1-\frac{2}{\rho}\right)\left[1+\rho^2\left\{\frac{H}{\rho^2} + \frac{3\lambda}{8}\left[\ln\left(1-\frac{2}{\rho}\right)\right.\right.\right.$$

$$\left.\left.\left. + \frac{2}{\rho}\left(1+\frac{1}{\rho}\right)\right]\right\}^2\right]. \tag{4.4}$$

This equation wherein the angular momentum term $d\phi/d\sigma$ has been eliminated in favour of the canonical angular momentum, H, expresses the effective energy conservation along the ρ-direction and may be written as

$$K^2 = \left(\frac{d\rho}{d\sigma}\right)^2 + V_{\text{eff}} \tag{4.5}$$

with

$$V_{\text{eff}} = \left(1-\frac{2}{\rho}\right)\left\{1+\rho^2\left[\frac{H}{\rho^2} + \frac{3\lambda}{8}\left\{\ln\left(1-\frac{2}{\rho}\right) + \frac{2}{\rho}\left(1+\frac{1}{\rho}\right)\right\}\right]^2\right\} \tag{4.6}$$

as the 'effective potential' in which the effective motion in the ρ coordinate occurs. The "turning points" of the motion are given by $d\rho/d\sigma = 0$. At these turning points $d\phi/d\sigma$ will be real only if

$$K^2 \geqslant \left(1 - \frac{2}{\rho}\right). \tag{4.7}$$

Since we are concerned with the motion for $\rho > 2$, this inequality is trivially satisfied for particles with $K \geqslant 1$. For $K < 1$ on the other hand we should have

$$\rho < \frac{2}{(1 - K^2)} \tag{4.8}$$

i.e., for non-relativistic particles we should consider only those turning points which lie in the region

$$2 < \rho < \frac{2}{(1 - K^2)}. \tag{4.9}$$

The character of the motion in the ρ-coordinate is determined completely by the effective potential V_{eff}. To begin with we can consider the following limiting behaviour of V_{eff}. For very large ρ, we can expand the logarithmic term and we get

$$V_{eff} = \left(1 - \frac{2}{\rho}\right)\left(1 + \frac{H^2}{\rho^2} + \ldots\right)$$

$$\simeq \left(1 - \frac{2}{\rho}\right) \tag{4.10}$$

Hence $\underset{\rho \to \infty}{\mathcal{L}t}\ V_{eff} = 1$.

On the other hand the behaviour of V_{eff} in the close neighbourhood of $\sigma \approx 2$ is governed essentially by the behaviour of the term $(1 - 2/\rho)\,[\ln(1 - 2/\rho)]^2$ and this tends to zero as $\rho \to 2$. Thus we have $\underset{\rho \to 2}{\mathcal{L}t}\ V_{eff} = 0$. It is indeed very interesting to see that even though the magnetic field components tend to infinity logarithmically as $\rho \to 2$, the effective potential tends to zero as $\rho \to 2$. In order to consider the behaviour of V_{eff} in general we first consider the extrema of the function V_{eff}, which we have tabulated in tables (1) to (4) for $H > 0$ and tables (5) and (6) for $H < 0$, for different values of λ.

Case 1: H > 0

We have found that in general there are two maxima and two minima the inner maximum (K_{M1}) minimum (K_{m1}) staying close to $\rho = 2$, whereas the outer minimum (flat) lies very far away roughly at $\rho \approx H^2$. We have presented in tables 1 to 4 the values of these extrema and their corresponding ρ values. It is important to notice that the two maxima move up and down as the values of H and λ vary. Figure A presents a typical plot of K_{M1}, K_{M2} and K_{m1} against H for a

Table 1. $H > 0$. $\lambda = 27{\cdot}5$.

H	K_{M_1}	ρ_{M_1}	K_{m_1}	ρ_{m_1}	K_{M_2}	ρ_{M_2}	K_{m_2}	ρ_{m_2}
17·6954	6·13	2·056	0·60	3·11	1·77	6·11	0·9984	305
21·2344	5·85	2·050	0·55	2·88	2·22	5·52	0·9989	444
24·7735	5·59	2·045	0·51	2·71	2·72	5·11	0·9992	607
31·5458	5·12	2·037	0·45	2·50	3·76	4·62	0·9995	989
34·4136	4·93	2·034	0·42	2·43	4·22	4·47	0·9996	1179
41·1247	4·52	2·028	0·37	2·32	5·35	4·21	0·9997	1686
70·7816	3·10	2·012	0·23	2·11	10·63	3·68	0·9999	5005
81·2964	2·72	2·009	0·20	2·08	12·57	3·58	0·9999	6605
99·5468	2·17	2·005	0·15	2·05	15·97	3·47	0·9999	9905

$K^2 = V_{\text{eff}}$. M = Maximum; m = minimum.

Table 2. $H > 0$. $\lambda = 50$.

H	K_{M_1}	ρ_{M_1}	K_{m_1}	ρ_{m_1}	K_{M_2}	ρ_{M_2}	K_{m_2}	ρ_{M_2}
17·6954	12·38	2·072	0·74	4·33	1·39	8·86	0·9984	302
21·2344	12·06	2·068	0·70	3·89	1·70	7·72	0·9989	441
24·7735	11·76	2·064	0·66	3·57	2·07	6·97	0·9992	604
31·5458	11·19	2·057	0·60	3·16	2·89	6·04	0·9995	987
34·4136	10·97	2·054	0·58	3·03	3·27	5·77	0·9996	1177
41·1247	10·45	2·048	0·54	2·81	4·22	5·28	0·9997	1684
70·7816	8·46	2·030	0·39	2·36	8·98	4·28	0·9999	5005
81·2964	7·86	2·025	0·35	2·28	10·79	4·10	0·9999	6604
99·5468	6·91	2·019	0·30	2·19	14·02	3·89	0·9999	9905

Table 3. $H > 0$. $\lambda = 100$.

H	K_{M_1}	ρ_{M_1}	K_{m_1}	ρ_{m_1}	K_{M_2}	ρ_{M_2}	K_{m_2}	ρ_{m_2}
17·6954	26·40	2·084	0·85	7·04	1·13	15·37	0·9984	307
21·2344	26·06	2·081	0·82	6·17	1·28	12·83	0·9989	445
24·7735	25·72	2·079	0·80	5·53	1·47	11·21	0·9992	607
31·5458	25·10	2·074	0·76	4·70	2·00	9·27	0·9995	981
34·4136	24·84	2·073	0·74	4·44	2·24	8·71	0·9996	1179
41·1247	24·24	2·068	0·71	3·98	2·92	7·72	0·9997	1686
70·7816	21·77	2·053	0·58	3·00	6·66	5·65	0·9999	5003
81·2964	20·96	2·048	0·54	2·83	8·18	5·29	0·9999	6602
99·5468	19·64	2·041	0·49	2·62	10·98	4·85	0·9999	9903

Table 4. $H > 0$. $\lambda = 250$.

H	K_{M_1}	ρ_{M_1}	K_{m_1}	ρ_{m_1}	K_{M_2}	ρ_{M_2}	K_{m_2}	ρ_{m_2}
17·6954	68·60	2·092	0·93	15·02	1·012	38·81	0·9985	330
21·2344	68·25	2·091	0·92	12·96	1·046	29·69	0·9989	463
24·7735	67·89	2·090	0·91	11·42	1·101	24·72	0·9992	624
31·5458	67·22	2·088	0·89	9·37	1·278	19·30	0·9995	1000
34·4136	66·94	2·087	0·88	8·73	1·381	17·78	0·9996	1192
41·1247	66·29	2·085	0·86	7·57	1·683	15·18	0·9997	1696
70·7816	63·48	2·076	0·79	5·07	3·802	9·88	0·9999	5009
81·2964	62·52	2·073	0·75	4·62	4·773	8·96	0·9999	6608
99·5468	60·88	2·070	0·73	4·05	6·698	7·80	0·9999	9908

Table 5.

	$\lambda = 27{\cdot}5$				$\lambda = 50$			
H	K_M	ρ_M	K_m	ρ_m	K_M	ρ_M	K_m	ρ_m
−17·6954	9·80	2·17	0·9984	315	16·03	2·13	0·9984	318
−21·2344	10·27	2·19	0·9988	452	16·45	2·14	0·9989	455
−24·7735	10·76	2·21	0·9992	614	16·88	2·15	0·9992	617
−31·5458	11·74	2·25	0·9995	995	17·74	2·17	0·9995	997
−34·4136	12·17	2·27	0·9996	1184	18·11	2·18	0·9996	1185
−41·1247	13·23	2·32	0·9997	1690	19·01	2·20	0·9997	1692
−70·7816	18·31	2·50	0·9999	5008	23·41	2·30	0·9999	5009
−81·2964	20·21	2·55	0·9999	6607	25·10	2·34	0·9999	6607
−99·5468	23·56	2·61	0·9999	9907	28·12	2·41	0·9999	9908

Table 6.

	$\lambda = 100$				$\lambda = 250$			
H	K_M	ρ_M	K_m	ρ_m	K_M	ρ_M	K_m	ρ_m
−17·6954	30·04	2·115	0·9984	326	72·25	2·104	0·9985	349
−21·2344	30·44	2·118	0·9989	462	72·62	2·106	0·9989	481
−24·7735	30·83	2·122	0·9992	623	73·00	2·107	0·9992	640
−31·5458	31·61	2·129	0·9995	1001	73·73	2·109	0·9995	1015
−34·4136	31·94	2·133	0·9996	1190	74·04	2·110	0·9996	1203
−41·1247	32·74	2·141	0·9997	1695	74·77	2·113	0·9997	1706
−70·7816	36·48	2·182	0·9999	5011	78·10	2·126	0·9999	5017
−81·2964	37·90	2·199	0·9999	6610	79·31	2·131	0·9999	6615
−99·5468	40·46	2·229	0·9999	9909	81·46	2·139	0·9999	9914

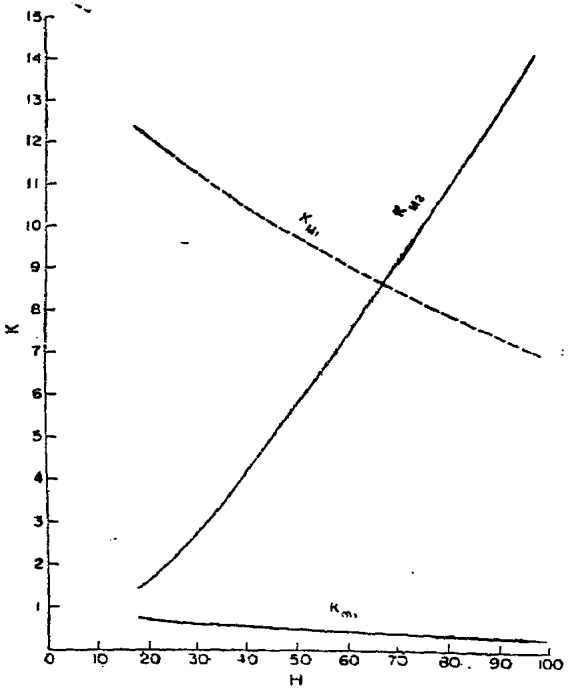

Figure A. Plots of V_{eff} maxima and V_{eff} minimum against the canonical angular momentum H, for the value of $\lambda = 50$. This is a typical plot and tables 1 to 4 for $H > 0$ and tables 5 and 6 for $H < 0$ show the actual behaviour of V_{eff} extrema which for a fixed λ would show the same trend as above.

given λ. As may be seen K_{M1} is a monotonic decreasing function of H whereas K_{M2} is monotonically increasing with H. There is always a value of H for which the two maxima are equal.

From the appearance of the extrema we can see that there are five sections for the curve V_{eff} vs ρ. Since we have seen that $V_{eff} \to 0$ as $\rho \to 2$, the function starts (i) increasing to the inner maxima very close to $\rho = 2$, (ii) falls sharply to the minimum; (iii) then increases towards the outer maximum and then (iv) starts decreasing towards $V_{eff} = 1$. (v) Very far from the source, V_{eff} dips below the value 1 to reach the outer minimum and finally tends to 1 asymptotically, as $(1 - 2/\rho)$.

We give here in figures 1, 2 and 3 a few plots of V_{eff} *vs* ρ for a few typical sets of values of H and λ. In view of the scaling difficulties the inner maximum and the outer minimum are not represented. As can be seen from the curves sections (ii) and (iii) represent the potential well. From figure A we have seen that for a given λ as H varies the two maxima vary and they are equal for a certain value of H. This H obviously corresponds to the value when the potential well has a maximum depth. From the structure of the potential curves it may be seen that there are four different classes of orbits for the particle.

(i) Highly relativistic particles with K^2 greater than the absolute maximum of V_{eff} (*e.g.*, $K = 7$, $H = 17{\cdot}6954$, $\lambda = 27{\cdot}5$) coming from infinity finds no barrier and plunges straight into the central star.

(ii) When K_{M1} is absolute (*e.g.*, $\lambda = 30$, $H = 24{\cdot}7735$) particles with energy such that $K_{M2} < K < K_{M1}$, have only unbound orbits as they would have only one turning point ($\lambda = 30$, $H = 24{\cdot}7735$, $K = 5$). On the other hand, particles with $1 < K < K_{M2}$ will have four turning points, of which the outermost corresponds to the unbound orbit, whereas the next two correspond to the envelopes of a gyrating orbit. Thus a particle coming from infinity with such an energy

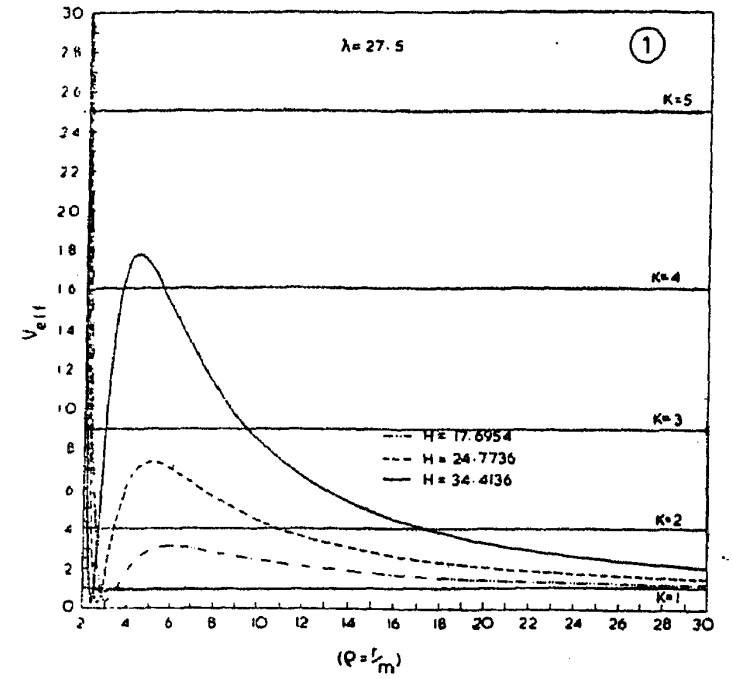

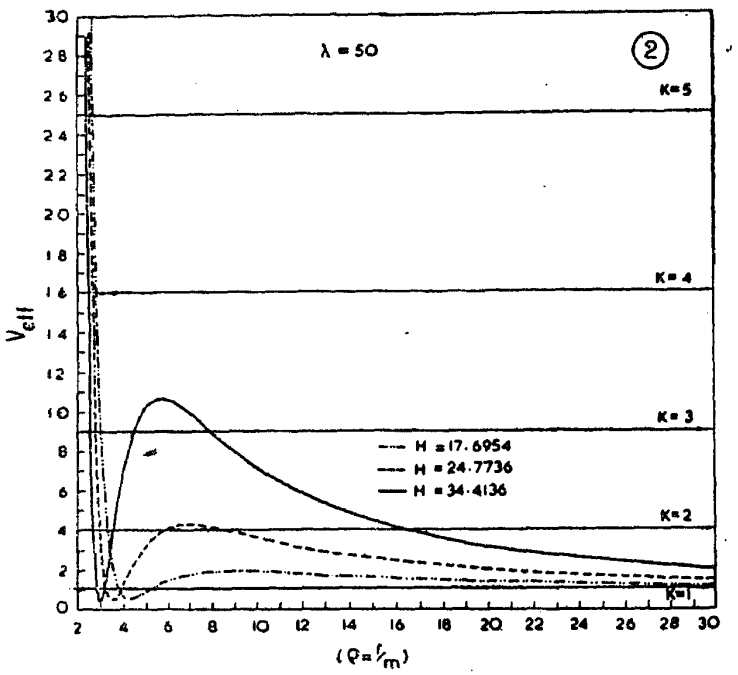

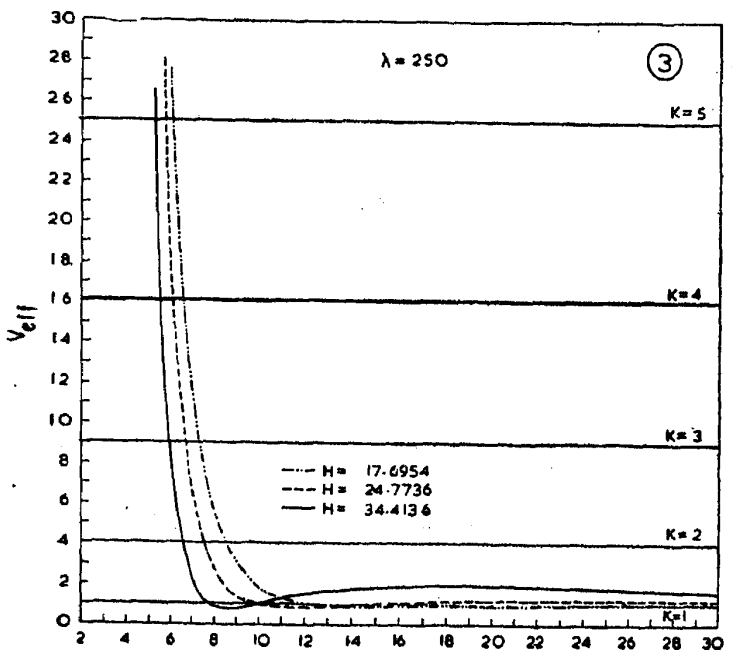

Figures 1, 2, 3. Plots of $V_{eff.}$ *vs* ρ for three different values of $H > 0$, for three different λ. The inner maximum and the outer minimum are beyond the reach of the scale used here As λ increases note the flattening of the potential well.

would turn back whereas those initially positioned at a value of ρ corresponding to the interior of the potential well, will gyrate in tightly bound orbits, *i.e.*, execute Larmor motion (figures 5 to 8).

(iii) When K_{M2} is absolute (*e.g.*, $\lambda = 30$, $H = 70{\cdot}7816$) particles with $K_{M1} < K < K_{M2}$, will have only unbound orbits whereas those with K such that $1 < K < K_{M1}$ shall have unbound orbit if it is coming from a far distance and bound orbit (Larmor motion) if it is inside the potential well (figure 9).

In both the above cases we thus have particles trapped around the central star if they have right type of energy and initial position.

(iv) Finally we have circular orbits corresponding to the extrema of the potential curve, the ones corresponding to maxima being unstable and the ones corresponding to minima being stable.

For a given value of H, as λ increases the potential curve flattens out, as the inner maximum rises and the outer maximum diminishes reducing the possibility of the particle trapping. In fact this feature may be qualitatively understood from the expression for $d\phi/d\sigma$,

$$\frac{d\phi}{d\sigma} = \frac{H}{\rho^2} + \frac{3\lambda}{8}\left\{\ln\left(1-\frac{2}{\rho}\right) + \frac{2}{\rho}\left(1+\frac{1}{\rho}\right)\right\},$$

which has to go through zero for gyrating orbits. Since the contributions from the H and λ terms are of opposite signs, fixing H and increasing λ arbitrarily, naturally reduces the possibilities of $d\phi/d\sigma$ becoming zero for lower values of ρ.

As mentioned in the beginning one finds from figure A that there is a certain combination of H and λ when the depth of the potential well is maximum for which combination the particle trapping is maximum.

Case 2: $H < 0$

Tables (5) and (6) show that there is only one maximum which is close to $\rho = 2$ and a flat minimum very far from the source. In this case, however, we have no trapping of particles in gyrating orbits as is clear from the expression for $d\phi/d\sigma$ which can never be zero ($d\phi/d\sigma$ is always negative). Figure 4 gives the plot of V_{eff} *vs* ρ which of course does show neither the maximum nor the minimum due to the scaling difficulty. Thus particles with very high energies would go into the central star and those with energies $K < K_M$ would scatter after being turned away by the field. As in the case of $H > 0$, there are circular orbits which are stable for nonrelativistic particles with $K = K_m < 1$, and unstable for relativistic ones with $K = K_M \gg 1$.

In general, the behaviour of the effective potential seems to be some kind of a combination of that in a pure magnetic field and in a pure gravitational field. In particular, the behaviour at large distances (for not too high magnetic field) seems not surprisingly, similar to that of particle motion in a pure Schwarzschild space-time $V_{eff} \approx 1 - 2/\rho + H^2/\rho^2$ as the outer minimum occurs at $\rho \approx H^2$. On the other hand, the first potential minimum close to the event horizon is characteristic of the gyrating orbits of particles in a pure magnetic field.

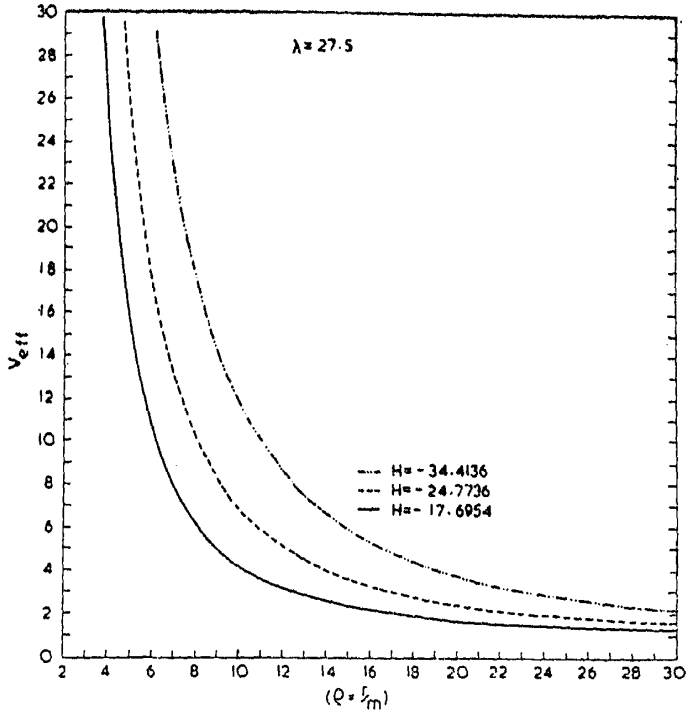

Figure 4. Plot of V_{eff}. *vs* ρ for three different values of $H < 0$. There is no potential well and thus no trapping of particles. The behaviour is just the same for other values of λ too.

5. Numerical integration of orbit equations

We next consider the numerical integration of the equations of motion to determine the precise forms of trajectories. The initial conditions for such an integration have to be appropriately chosen. We thus consider briefly the manner in which these initial conditions are picked.

Case (a): Equatorial plane

The equation to be integrated are those given by (4.1) to (4.3). For this we need initially, apart from the values of the physical parameters, K and λ, the velocities $(d\rho/d\sigma)_0$ $(d\phi/d\sigma)_0$ and the initial position ρ_0 and ϕ_0. In the case of bound orbits, since the particle executes Larmor motion, we should have $d\phi/d\sigma = 0$ at some $\rho = \rho_0$. We thus choose initially $(d\phi/d\sigma)_0 = 0$ at $\rho = \rho_0$. This gives us from (4.2)

$$H = -\frac{3\lambda\rho_0^2}{8}\left\{\ln\left(1-\frac{2}{\rho_0}\right)+\frac{2}{\rho_0}\left(1+\frac{1}{\rho_0}\right)\right\} \tag{5.1}$$

and

$$\left(\frac{d\rho}{d\sigma}\right)_0 = \sqrt{K^2-1+2/\rho_0} \tag{5.2}$$

from (4.3). Thus now specifying λ, K, ρ_0 and ϕ_0 we have all the necessary initial values. We choose always $\phi_0 = 0$.

We have considered a number of cases but presented a few typical cases here (figures 5 to 9). We find that for a given λ, as the initial position tends closer to the event horizon the Larmor circle gets smaller and flatter inside. This feature is probably due to the effects of curvature on the magnetic field.

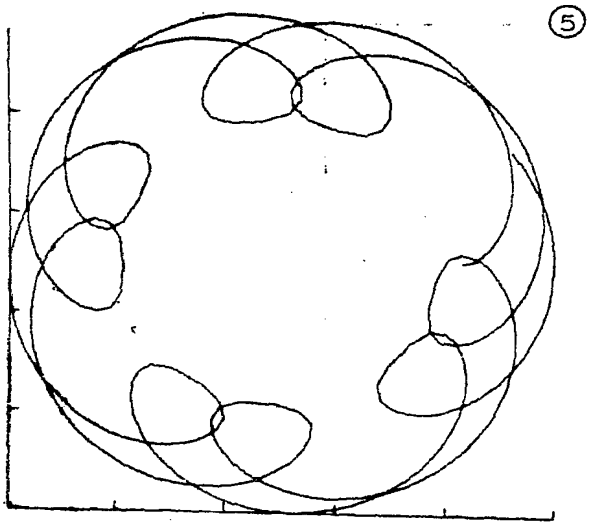

K=2, λ=30, ρ_0=3, H=21·2345

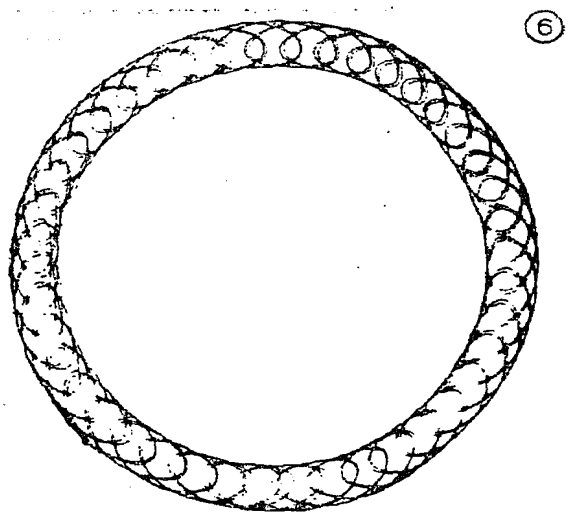

K=2, λ=30, ρ_0=2·5, H=34·4136

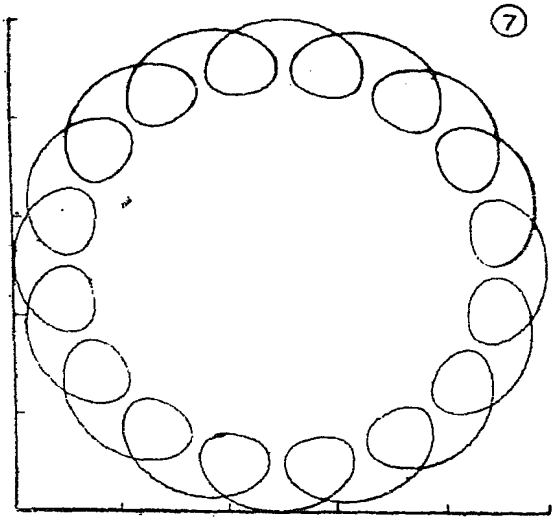

K=2, λ=100, ρ_0=4, H=40·8883

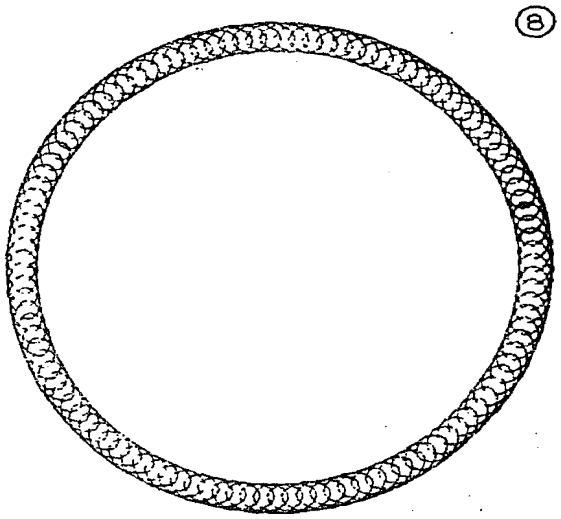

K=2, λ=100, ρ_0=3, H=70·7816

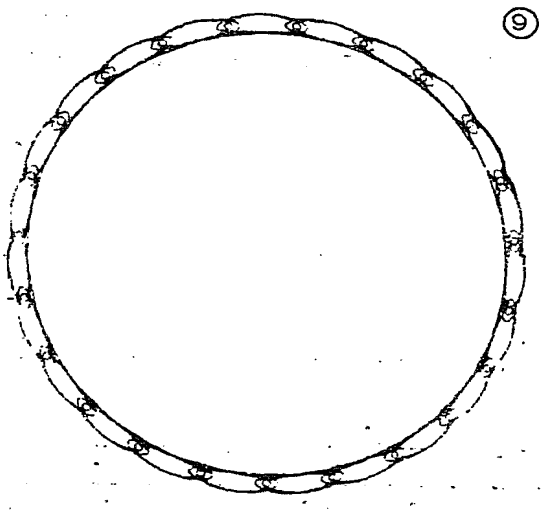

K=3, λ=30, ρ_0=2·1, H=81·2964

Figures 5, 6, 7, 8, 9. Equatorial plane view of the orbits of a positively charged particle in a dipole magnetic field on the Schwarzschild background, the magnetic field itself being modified by the curvature of space-time. The various physical parameters are indicated in the figures. The turning points which correspond to the envelopes of the gyrating orbits are as follows:

(5) $\rho_{min} = 2{\cdot}562$ $\rho_{max} = 4{\cdot}560$, (6) $\rho_{min} = 2{\cdot}300$ $\rho_{max} = 2{\cdot}829$, (7) $\rho_{min} = 3{\cdot}526$ $\rho_{max} = 4{\cdot}987$, (8) $\rho_{min} = 2{\cdot}834$ $\rho_{max} = 3{\cdot}220$, (9) $\rho_{min} = 2{\cdot}023$ $\rho_{max} = 2{\cdot}195$.

Case (b) : Motion along the field lines

In order to consider the motion along the field lines we need to consider the θ motion as well. We have to integrate the system of eqs (3.7) to (3.9). For initial conditions we again choose

$$\left(\frac{d\phi}{d\sigma}\right)_0 = 0 \text{ at } \rho = \rho_0, \ \theta_0 = \pi/2 \tag{5.3}$$

so that we have

$$H = -\frac{3\lambda\rho_0^2}{8}\left[\ln\left(1-\frac{2}{\rho_0}\right) + \frac{2}{\rho_0}\left(1+\frac{1}{\rho}\right)_0\right] \tag{5.4}$$

and

$$\left(\frac{d\rho}{d\sigma}\right)_0^2 = K^2 - \left(1-\frac{2}{\rho_0}\right)\left\{1+\rho_0^2\left(\frac{d\theta}{d\sigma_0}\right)^2\right\}. \tag{5.5}$$

We need to specify $(d\theta/d\sigma)_0$ or $(d\rho/d\sigma)_0$. From (5.5) we get for $(d\rho/d\sigma)_0$ to be real, the condition on $(d\theta/d\sigma)_0$ to be

$$\left(\frac{d\theta}{d\sigma}\right)_0^2 < \left[\frac{K^2}{\rho_0^2}\left(1-\frac{2}{\rho_0}\right)^{-1} - \frac{1}{\rho_0^2}\right]. \tag{5.6}$$

Thus specifying λ, K, ρ, and $(d\theta/d\sigma)_0$ say, we can integrate the system of eqs (3.7) to (3.9) and obtain the orbits. Figure 10 presents a typical case of the motion along the field lines. As may be seen from the figure, the features are essentially same as in the case of a pure magnetic field in that the particle gyrates in a given tube of lines reflecting between two mirror points, if the magnetic field is sufficiently large, and the initial velocity in the direction small. When the magnetic field is lower, the particle oscillates up and down the $\theta = \pi/2$ plane for a while till the ρ value reaches a certain minimum at which the particle moves continuously towards the central star. However a more general analysis has not

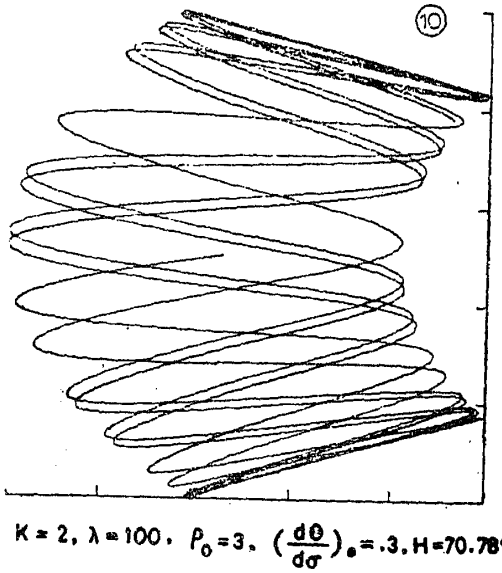

Figure 10. Projection of the (ρ, θ) motion of positively charged particle indicating the reflection at mirror points; the particle executes an oscillatory motion characteristic of the motion in a magnetic field.

been possible in this case as we did for the case of motion in the equatorial plane.

6. Conclusions

We have found that the presence of a magnetic field on the Schwarzschild geometry alters the character of the motion considerably. The orbits which are spiralling in the purely gravitational case are now turned around by the magnetic field (as in the nonrelativistic case) and are thus stopped from spiralling in or out, and are trapped in a region of the r-space determined by the radius of gyration. In this sense the magnetic field seems to stabilize the originally unstable orbits.

The character of the motion in the combined gravitational and magnetic field is determined essentially by the behaviour of the effective potential V_{eff} as a function of r as discussed in section 4. As shown there the presence of the magnetic field results in an additional potential minimum bounded by two maxima. The trapping of the particle in this potential minimum corresponds to the gyration of the particle in the magnetic field. The positions of the maxima correspond to unstable circular orbits, while that of the minimum, to stable circular orbits. At large distances from the central body the effective potential approaches that due to the pure gravitational field because the magnetic field decreases faster than what the gravitational field does. Even though the effective potential tends to zero as $r \to 2m$ the fact that the components of the electromagnetic field tensor go to infinity invalidates the weak field formalism at the event horizon.

As already pointed out, the determination of the orbits in the combined magnetic and gravitational field is a first step towards the study of plasmas under these conditions. Discs of plasmas have been considered around condensed objects to provide a model for radio objects for x-ray sources and for pulsar radiation mechanism. A more systematic study of the plasmas in these situations need to be carried out than has hitherto been done.

Acknowledgements

It is a pleasure to thank Rao S Koneru for his valuable help in all the numerical computations. We would also like to thank V B Sheorey for his help in some of the computations.

References

Ginzburg V L and Ozernoi I M 1965 *Sov. Phys. JETP* **20** 689
IAU Symposium 64 1974 ed. C. Dewitt, (Reidel Publishing Company)
Petterson J A 1974 *Phys. Rev.* **D10** 3166
Stewart J and Walker M 1973 *Astrophysics Springer tracts in Mod. Phys.* **69** 89
Thorne K S and Novikov I 1972 *Black Hole Astrophysics in Black Holes*, eds Dewitt and Dewitt (Gordon and Breach)
ter Harr D 1972 *Phys. Rep.* **C3** 57
Zeldovich Ya B and Novikov I 1971 *Relativistic Astrophysics*, Vol. 1 (Univ. Chicago Press)